An optical (Q)PSK-RF-signal transmitter based on two cascaded Mach–Zehnder modulators

Tong Ye *, Cishuo Yan, Qingjiang Chang, Yikai Su

State Key Laboratory of Advanced Optical Communication Systems and Networks, Department of Electronic Engineering, Shanghai Jiao Tong University, Shanghai 200240, China

ARTICLE INFO

ABSTRACT

This paper proposes an optical transmitter to generate phase-shift-keying (PSK) radio frequency (RF)-signal, using two cascaded single-drive Mach–Zehnder modulators (SDMZMs). With input of a continuous-wave (CW) light, an electrical non-return-to-zero (NRZ) data, and an RF-local oscillator (RF-LO) signal at a frequency of ω_l, the transmitter can simultaneously produce three PSK signals and two CW tones on both sides in spectrum, by employing nonlinear modulation technique. With the help of optical filters, the desired signals can be selected to mix at a photodetector (PD) to obtain a PSK-RF-signal with the carrier frequency of ω_l, $3\omega_l$, or $5\omega_l$. Our scheme can be easily extended to generate quadrature PSK-RF-signal. The feasibility of our proposal is experimentally and numerically verified.

© 2008 Elsevier B.V. All rights reserved.

1. Introduction

Optical transmitter for radio-frequency (RF)-signal generation and distribution is important to the emerging radio-over-fiber (RoF) systems. The transmitter is required to modulate the data, such as phase-shift-keying (PSK) signal, onto the generated RF carrier.

Several schemes have been developed [1–3] to directly modulate the electrical phase of an RF-signal in the optical domain, where an expensive high-frequency RF-local oscillator (RF-LO) is indispensable. A PSK-subcarrier modulator was constructed in [4] utilizing a dual-drive Mach–Zehnder modulator (MZM). In that system, the frequency requirement on the RF-LO was relaxed as the carrier-frequency doubling technique was used, but the modulating data-rate was limited since the data was loaded to the MZM through the direct current (DC) bias port. A dual-mode PSK modulation method was proposed in [5], which required an electrical RF mixer to produce an electrical signal with a phase modulation of ±45° before the frequency doubling of the carrier in the optical domain. In [6], a special heterodyne subcarrier source (HSS) was employed to generate two coherent continuous-wave (CW) lights, which were firstly separated and then recombined to get mixed at the photodetector (PD) after one CW light was phase modulated. However, for such a heterodyning technique, separate transmission of the two lightwaves through different paths could make the phase of the generated signal unstable.

To address the aforementioned issues, we propose an optical RF transmitter, which produces a PSK signal and a CW tone simultaneously from an input CW light, and uses self-heterodyning to generate a PSK-RF-signal. The frequency of the RF carrier is determined by the frequency difference between the PSK signal and the CW tone, which is achieved by frequency multiplication of an RF-LO signal. Furthermore, generation of all the signal components without separate transmission guarantees the phase-stability of the PSK-RF-signal. Our preliminary scheme has been reported in [7], where an MZM cascaded by a dual-parallel MZM (DPMZM) is used to produce the PSK-RF-signal, whose carrier frequency is generated by doubling or quadrupling the RF-LO signal. To reduce the system complexity while obtain a higher carrier frequency compared to that in [7], we design a simple method in this paper, where two single-drive MZMs (SDMZMs) are employed. This method can be extended to create a quadrature PSK (QPSK) RF-signal by replacing the first SDMZM with a DPMZM.

2. Principle and schematic setup

As illustrated in Fig. 1, our scheme mainly employs two cascaded x-cut SDMZMs. An electrical non-return-to-zero (NRZ) data and an RF-LO signal are combined together and fed to the RF input of the first MZM. Suppose that the RF-LO signal is $S_l = \alpha_l \cos(\omega_l t + \phi_l)$, and the NRZ signal is $S_{NRZ} = \alpha_n b_n(t)$, where α_l and ω_l are the amplitude and frequency of the RF-LO signal respectively, α_n is the amplitude of the NRZ signal, and $b_n(t) = 1$ or -1, depending on the pseudo-random binary sequence (PRBS) generated by the pulse pattern generator (PPG) in Fig. 1. If the MZM is biased at its transmission null of V_π, the electrical field at the output of the first MZM is

$$E_{out}^1 = E\cos(wt)\cos\left[\frac{\pi}{2V_\pi}(S_l + S_{NRZ} + V_\pi)\right]$$
$$= -E\cos(wt)\sin\left[\frac{\pi}{2V_\pi}(S_l + S_{NRZ})\right],$$

* Corresponding author. Tel.: +86 21 3420 4602; fax: +86 21 3420 4370.
E-mail address: yetong@sjtu.edu.cn (T. Ye).
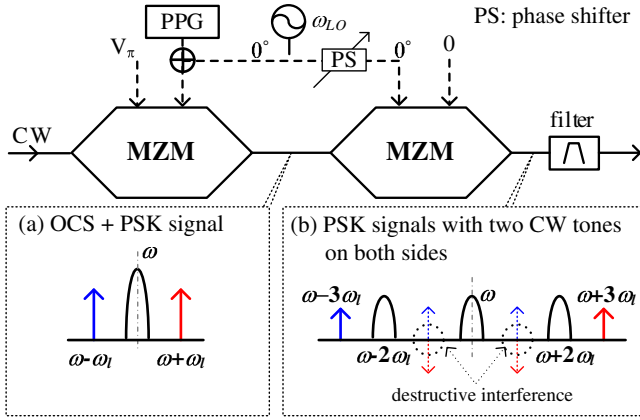
Fig. 1. Principle of the generation of PSK modulated radio frequency signals: (a) simultaneous optical carrier suppressed modulation and PSK modulation by the MZM, (b) three PSK signals with two CW tones on both sides.

Fig. 2. Principle of the generation of QPSK modulated radio frequency signals: (a) simultaneous OCS modulation and PSK modulation by the MZM, (b) QPSK signal and two CW tones, (c) three QPSK signals with two CW tones on both sides.

where E and ω are the amplitude and the frequency of input CW light, respectively. Substituting S_{NRZ} and S_l into the equation and using the triangle identical equalities, we then have

$$E^1_{\text{out}} = -E\cos(wt) \times \{\sin[x_l \cos(\omega_l t + \phi_l)]\cos[x_n b_n(t)] + \cos[x_l \cos(\omega_l t + \phi_l)]\sin[x_n b_n(t)]\},$$

where $x_l = \alpha_l\pi/2V_\pi$ and $x_n = \alpha_n\pi/2V_\pi$. Clearly, in the above equation, $\cos[x_n b_n(t)] = \cos x_n$ is a constant, whereas $\sin[x_n b_n(t)] = b_n(t)\sin x_n$ is time-variable. Using the Bessel function, we can expand the equation as follows:

$$E^1_{\text{out}} = -E\cos(wt)$$
$$\times \left\{ 2\cos x_n \times \sum_{n=1}^{\infty}(-1)^n J_{2n-1}(x_l)\cos[(2n-1)(\omega_l t + \phi_l)] \right.$$
$$\left. + \left[J_0(x_l) + 2\sum_{n=1}^{\infty}(-1)^n J_{2n}(x_l)\cos 2n(\omega_l t + \phi_l)\right] \times b_n(t)\sin x_n \right\},$$

where $J_i(\cdot)$ is the coefficient of the Bessel function. By adjusting the value of α_l (i.e., x_l) such that the high-order harmonics in the equation can be ignored, as shown in Fig. 1a, we can obtain one PSK signal and two CW tones on both sides

$$E^1_{\text{out}} \approx -E\cos(wt) \times [J_0(x_l)b_n(t)\sin x_n - 2J_1(x_l)\cos x_n \cos(\omega_l t + \phi_l)]$$
$$= -E\{J_0(x_l)\sin x_n \cos(\omega t + \phi_n)$$
$$- J_1(x_l)\cos x_n \cos[(\omega \pm \omega_l)t \pm \phi_l]\}, \tag{1}$$

where ϕ_n changes between 0 and π with the data stream at the RF input of the MZM. The generation of two CW tones is also known as optical carrier suppressed (OCS) modulation [8].

The output of the first MZM then enters the second MZM driven by the RF-LO signal $S'_l = \alpha'_l \cos(\omega_l t + \phi'_l)$. If the second MZM is biased at its transmission peak, the output signal is as follows:

$$E^2_{\text{out}} = E^1_{\text{out}}\cos\left[\frac{\alpha'_l\pi}{2V_\pi}\cos(\omega_l t + \phi'_l)\right]$$
$$= E^1_{out}\left\{J_0(x'_l) + 2\sum_{n=1}^{\infty}(-1)^n J_{2n}(x'_l)\cos 2n(\omega_l t + \phi'_l)\right\},$$

where $x'_l = \alpha'_l\pi/2V_\pi$. It is shown that, the second MZM generates one zero-order and a set of even-order harmonics for each input frequency component from the first MZM. If the value of α'_l is fine tuned such that $x'_l \approx 1.5$, for each optical component from the first MZM, the zero-order and two second-order harmonics will have the same amplitude (i.e., $J_0(1.5)/2 \approx J_2(1.5) \approx 0.256$), while the high-order harmonics can be ignored (e.g., $J_4(1.5) < 0.01$). For exam-

ple, as illustrated in Fig. 1b, as to the tone at $\omega - \omega_l$, the MZM creates three harmonics at $\omega - 3\omega_l$, $\omega - \omega_l$, and $\omega + \omega_l$. In this case, the output of the second MZM can be mathematically expressed as

$$E^2_{\text{out}} \approx -AJ_0(1.5)\cos(\omega t + \phi_n) + 2AJ_2(1.5)$$
$$\times \cos[(\omega \pm 2\omega_l)t + \phi_n \pm 2\phi'_l] + BJ_0(1.5)\cos[(\omega \pm \omega_l)t \pm \phi_l]$$
$$- 2BJ_2(1.5)\cos[(\omega \pm \omega_l)t \mp \phi_l \pm 2\phi'_l]$$
$$- 2BJ_2(1.5)\cos[(\omega \pm 3\omega_l)t \pm \phi_l \pm 2\phi'_l], \tag{2}$$

where $A = EJ_0(x_l)\sin x_n$, $B = EJ_1(x_l)\cos x_n$, and $J_0(1.5)/2 \approx J_2(1.5) \approx 0.256$.

Moreover, if $|\phi_l - \phi'_l| = k\pi (k = 0, 1, 2, \ldots.)$, Eq. (2) changes to

$$E^2_{\text{out}} \approx -0.512A\cos(\omega t + \phi_n) + 0.512A\cos[(\omega \pm 2\omega_l)t + \phi_n \pm 2\phi_l]$$
$$- 0.512B\cos[(\omega \pm 3\omega_l)t \pm 3\phi_l]. \tag{3}$$

This result indicates that if two RF-LO signals in phase are used to drive both MZMs, at the output of the second MZM, we can have three PSK signals spaced by $2\omega_l$ as well as two CW tones on both sides, which is illustrated in Fig. 1b. These five components are coherent to each other, since all of them originate from a same source without separated transmission. This is important to ensure the stability of the phase of the generated PSK-RF-signal.

By using the optical filters at the second MZM output, one can select a PSK signal and a CW tone. When an optical PSK signal mixes with a coherent CW signal at the PD, a PSK modulated electrical-carrier signal is produced, and the frequency of the carrier is determined by the spacing between the PSK signal and the CW tone [6]. The PSK signal at $\omega - 2\omega_l$ and the CW signal at $\omega + 3\omega_l$ are sent to the PD, a PSK modulated carrier at a frequency of $5\omega_l$ can be obtained. Similarly, the PSK signal at ω and $\omega + 2\omega_l$ mixing with the CW at $\omega + 3\omega_l$ leads to the PSK modulated carriers with the frequencies of $3\omega_l$ and ω_l, respectively.

Note that, this scheme can be easily extended to generate the QPSK-RF-signal in the similar way, if the first MZM in Fig. 1 is replaced by a DPMZM. Such extension is displayed in Fig. 2. Each arm of the DPMZM creates a PSK signal and two CW tones (see Fig. 2a). By controlling the bias of the main MZM of the DPMZM, we can obtain a QPSK signal and two CW tones in Fig. 2b, which are nonlinearly modulated by the following MZM to produce three QPSK signals with two CW tones on both sides, as shown in Fig. 2c.

3. Optical power budget

There are two types of optical losses in the system. On one hand, five strong components as well as undesired high-order harmonics are produced from an input CW light. Without any power compen-

sation, the energy of the CW light is distributed to all the generated harmonics. As described in Section 2, only two frequency components are used to produce the desired PSK-RF-signal, which inevitably incurs the power loss. On the other hand, there exists an inserting losses when the optical signals pass through optical components.

According to Eq. (3), after the two cascaded MZMs, each PSK component has the power of $|0.512A|^2$, that is,

$$P_{PSK} \approx |0.512EJ_0(x_l)\sin x_n|^2.$$

Similarly, we can obtain the power of each CW tone as follows:

$$P_{CW} \approx |0.512EJ_1(x_l)\cos x_n|^2.$$

Then the power losses due to the generation of undesired high-order harmonics can be estimated as follows:

$$L_A^h \approx -10\log_{10}\left(\frac{3P_{PSK} + 2P_{CW}}{|E|^2}\right)$$
$$= -10\log_{10}\left\{0.512^2 \times \left[3J_0^2(x_l)\sin^2 x_n + 2J_1^2(x_l)\cos^2 x_n\right]\right\}. \quad (4)$$

Once a PSK signal and a CW tone are selected by the optical filter, the loss will be

$$L_A \approx -10\log_{10}\left(\frac{P_{PSK} + P_{CW}}{|E|^2}\right). \quad (5)$$

Suppose that the insertion losses of the MZM and the optical filters are L_I^M and L_I^F, respectively. The total insertion loss is $L_I = L_I^M + L_I^F$, and the total system loss can be calculated as

$$L = L_A + L_I. \quad (6)$$

4. Experimental results

The experimental setup is given in Fig. 3. The data generated by the PPG is a 1.25-Gb/s PRBS with a word length of $2^7 - 1$. The employed 10-GHz SDMZMs (JDSU OC-192) have a V_π of 5.5 V, a rated input optical power is 10 dBm, and an insertion loss of 6 dB. A 20-GHz microwave synthesizer (Agilent E8257D) is used to generate a sine wave at a frequency of 10 GHz, which is split up into two branches and fed to the RF ports of two MZMs. These two RF-signals are kept in phase by employing a tunable RF phase shifter. To select the desired frequency components, two fiber Bragg gratings (FBGs) are used as the optical fibers. One wide-band FBG has a bandwidth of ∼0.25 nm (or ∼30 GHz) is mechanically tunable, while the other one with a bandwidth of ∼0.11 nm (or ∼14 GHz)

Fig. 3. Experimental setup. Note that the gray part is for the simulation. TOF: tunable optical filter; VOA: variable optical attenuator; OC: optical circulator; PC: polarization controller; LPF: low-pass filter.

is fixed. To demodulate the PSK signal, a 5-GHz Mach–Zehnder delay interferometer (MZDI) is deployed, which is home made using two 3-dB 2 × 2 optical couplers.

Due to the power losses as analyzed in Section 3, two erbium-doped fiber amplifiers (EDFAs) are included in the system to compensate the optical losses.

4.1. PSK-RF-signal generation

A 6-dBm CW light is injected into the system. Initially, only the 10-GHz RF-LO signal with a peak-to-peak voltage of $V_{pp} \approx 4.8$ V is applied to the first MZM biased at V_π. Observed from Fig. 4a, we obtain an OCS signal with a suppression ratio of other harmonics more than 20 dB. Note that, the resolution of the optical spectrum analyzer (Anritsu MS9710B) used to observe the optical spectrum is 0.07 nm. When the RF-LO signal is combined with the 1.25-Gb/s NRZ data with $V_{pp} \approx 5.5$ V, a PSK signal appears between two CW tones of the OCS signal as plotted in Fig. 4b. The combination of the PSK and OCS signals has a power of −2 dBm. In particular, the power of the PSK signal in Fig. 4b is about −3.2 dBm. It is then amplified to 8 dBm and fed into the second MZM, which is driven by the 10-GHz RF-LO signal with $V_{pp} \approx 10.5$ V. To obtain such high-power RF-signal, we have to employ a narrow-band high-power RF amplifier (Endwave JCA910-3182), which will be unnecessary if an MZM with a small V_π is available. Actually, the single-drive MZM with $V_\pi < 3$ V, such as Fujitsu FTM7928FB, has been commercial. It is evident in Fig. 4c that the second MZM produces five strong peaks in the frequency domain. To facilitate the explanation, we mark the frequency components with (1)–(5) sequentially from the left to right. It is exhibited in Fig. 4c that (2), (3), and (4) each shows a power of −5 dBm, which is 10-dB higher than (1) (or (5)).

In the following, we demonstrate that (2), (3), and (4) are PSK signals, while (1) and (5) are CW tones. Firstly, we select (3) in Fig. 4d, using the narrow-band FBG. Fig. 4e and f gives the corresponding optical eye-diagrams of the signal and demodulated signal, respectively, which verify that (3) is a 1.25-Gb/s PSK signal. Note that, since the suppression ratio of the FBG is not high enough, Fig. 4e and f exhibits that there is a high-frequency component (∼20 GHz) in the waveform. Fortunately, it does not affect the PD to perform data recovery from the optical signal, as indicated by the electrical eye-diagram of the PSK signal in Fig. 4g. To show (4) is a PSK signal, we also filter out (3) and (4) in Fig. 4h, employing the wide-band FBG. Fig. 4i displays the beating result of (3) and (4). The waveform in Fig. 4i is a 20-GHz clock, where the amplitude and the frequency keep almost unchanged. This confirms that (4) is a PSK signal, which always keeps in-phase with (3). We use the 14-GHz FBG to select the PSK signal (4) and the CW tone (5). The central wavelength of the FBG is located close to (5) such that (3) can be sufficiently suppressed, as plotted in Fig. 4j. Due to the optical filtering, the power of the PSK signal (4) is reduced to −7 dBm. After (4) and (5) are mixed in the PD, we observe a 10-GHz RF-signal modulated by a 1.25-Gb/s PSK data in Fig. 4k, where the duration of one bit of the data is 800 ps and the phase transition of the carrier happens between '0' and '1' bits. This indicates that (5) is a CW light. In the similar way, we can prove that (1) and (2) are CW light and PSK signal, respectively. It is straightforward to envision that a 50-GHz or 30-GHz signal with a 1.25-Gb/s PSK modulation can be obtained if (2) or (4) beats with (5). However, we can not filter out (3) and (5), or (2) and (5), simultaneously, since we lack enough FBGs.

We demonstrate the generation of 30-GHz and 50-GHz PSK-RF-signals through simulations using the software by VPIsystem. To generate the 30-GHz PSK-RF-signal, we use several FBGs to filter out frequency components (1), (2), (4) in Fig. 4c. For example, we use two FBGs, which have a bandwidth of 18 GHz and a reflection ratio of 30 dB, to reflect component (4). Fig. 5a gives the electrical
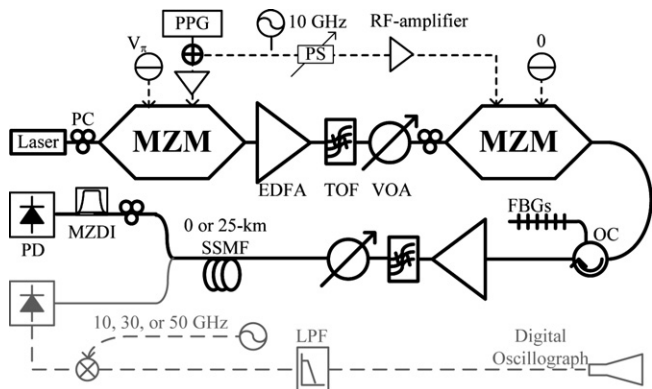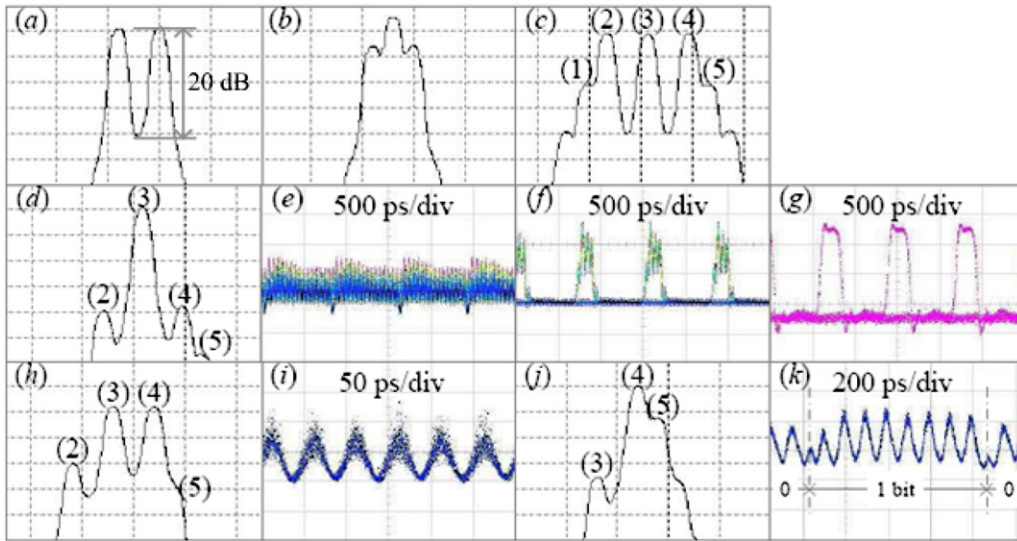
Fig. 4. Experimental results: optical spectra (x: 0.2 nm/div and y: 5 dB/div) and waveforms: (a) OCS modulation in the first MZM; (b) PSK and OCS signals produced by the first MZM; (c) five-peak signal generated by the second MZM, where (2), (3), and (4) are PSK signals and (1) and (5) are CW tones; (d) filtered central PSK signal; (e) optical eye-diagram of central PSK signal; (f) optical eye-diagram of demodulated central PSK signal; (g) electrical eye-diagram of demodulated central PSK signal; (h) spectra of PSK signal and CW tone on the right; (i) electrical eye-diagram of 20-GHz clock; (j) spectra of PSK signals (3) and (4); (k) electrical waveform of the 10-GHz PSK-RF-signal.
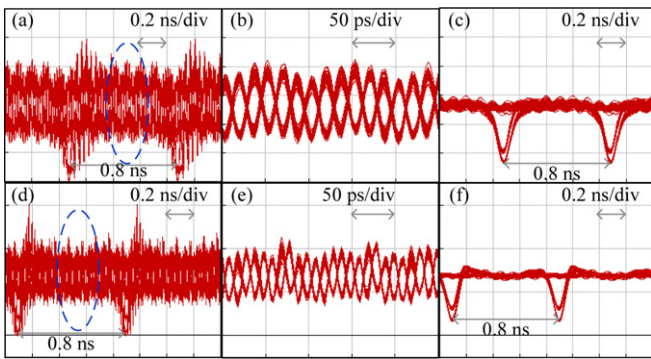
Fig. 5. Simulation results for the generation of 30-GHz and 50-GHz PSK-RF-signal: (a) electrical eye-diagram of the 30-GHz PSK-RF-signal; (b) magnified picture of the RF carrier in the blue circle in (a); (c) the PSK envelope; and (d)-(f) are the corresponding results for the 50-GHz case.

eye-diagram of the RF-signal. It shows that there is a residual amplitude modulation, mainly induced by the optical filtering. To look into the RF carrier, the eye-diagram in the circle is magnified in Fig. 5b. The observation confirms that the frequency of the RF carrier is 30 GHz and the phase-shift between "0" and "1" bits is about π. We then use a 5-GHz electrical low-pass filter to remove the RF carrier, and a 1.25-GHz PSK envelop is clearly shown in Fig. 5c. Similar results for the generation of 50-GHz PSK-RF-signals are also presented in Fig. 5d–f, which verify the feasibility of the scheme.

4.2. Transmission performance

In a typical RoF system, the generated optical RF-signal, consisting of a PSK signal and a CW tone, is delivered from the central station to the remote base stations, where it is converted into an electrical wireless signal and broadcast through air. Hence, we evaluate the transmission performance of the output signal for the remote data distribution.

We firstly test the transmission performance of the baseband PSK signal, by transmitting the signal at (3) in Fig. 4 over a 25-km standard single mode fiber (SSMF). The peak of the signal is selected by the narrow-band FBG and preamplified by the EDFA. After the 25-km transmission, it is demodulated by the MZDI and detected by a 10-GHz PD. Fig. 6 shows the measured BER performance, a power penalty of ~1 dB is observed. Such a large penalty is incurred by the imperfections of the home made MZDI. Its high sensitivity to the temperature and vibration makes the measurement inaccurate. If an integrated MZDI were available, the power penalty would be possibly reduced significantly.

In the following, we evaluate the transmission performance of the PSK-RF-signal through simulation. Suppose that the selected PSK signals and CW tone are at the frequencies of ω_p and ω_c and have the optical powers of P_p and P_c, respectively. When they are fed to a PD with a responsivity of R, one can obtain the detected photocurrent as

$$i = R\left[P_p + P_c + 2\sqrt{P_p P_c}\cos\left(|\omega_p - \omega_c|t + \phi_n\right)\right],$$
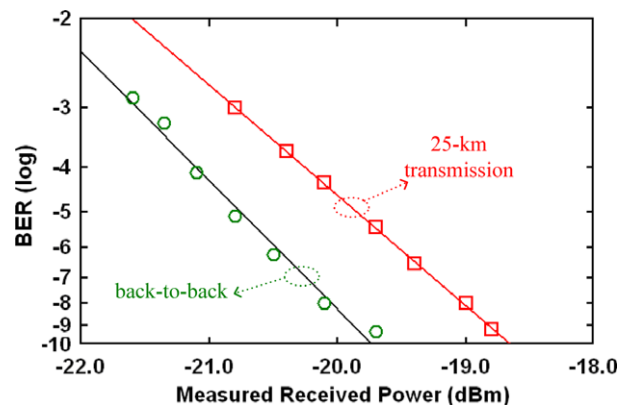
Fig. 6. Bit-error-rate performance of baseband PSK signal with and without 25-km transmission.
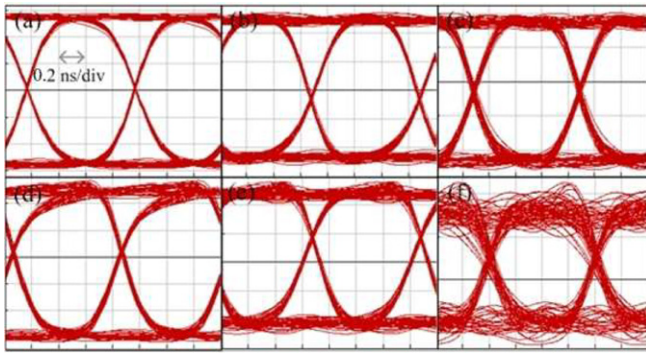
Fig. 7. The electrical eye-diagrams of the baseband signals down-converted from (a) 10-GHz, (b) 30-GHz, and (c) 50-GHz PSK-RF-signals without transmission; (d)–(f) are the corresponding eye-diagrams after the 25-km transmission.

where the phase of the CW signal is assumed to be zero for the convenience. As shown in Fig. 4, the electrical signal is then mixed with a coherent RF-signal at a frequency of $\omega_{RF} = |\omega_p - \omega_c|$, and filtered by an LPF with a 3-dB bandwidth of 1.25 GHz. Thus, one can get the baseband signal as follows:

$$i_{BS} = 2R\sqrt{P_p P_c}\cos\phi_n = \pm 2R\sqrt{P_p P_c}.$$

The transmission performance evaluation of the PSK-RF-signal can be achieved by comparing the eye-diagrams of the baseband signals before and after transmission, which are given in Fig. 7. It shows that, after the 25-km transmission, the 10-GHz RF-signal has the least distortion, the 50-GHz RF-signal suffers the most degradation, and the 30-GHz RF-signal is in between. This is attributed to the dis-persion of the 25-km SSMF with a group velocity dispersion of 17 ps/nm/km.

5. Conclusion

This paper proposes an optical PSK-RF-signal transmitter based on nonlinear modulation technique, using two cascaded MZMs. With the input of an RF-LO signal ω_l and an electrical NRZ data, the transmitter is able to produce a PSK modulated RF-signal at a frequency up to $5\omega_l$. Our discussion shows that this scheme can be easily extended for the generation of QPSK-RF-signal. We demonstrate the feasibility of the RoF transmitter through the experiments and simulations.

Acknowledgements

References

[1] S. Fukushima, Y. Doi, T. Ohno, H. Takeuchi, IEEE Photon. Technol. Lett. 11 (1999) 1036.
[2] M. Shin, J. Lim, C.Y. Park, J. Kim, J.S. Kim, K.E. Pyun, S. Hong, IEEE Photon. Technol. Lett. 12 (2000) 516.
[3] A. Loayssa, D. Benito, Electron. Lett. 40 (2004) 1362.
[4] A. Martínez, V. Polo, J.L. Corral, J. Martí, IEEE Photon. Technol. Lett. 15 (2003) 772.
[5] Y. Ozeki, M. KiShi, A. Tsuchiya, in: Proc. Microwave Photon. Proc. MWP, Paper Tu-25, 2001.
[6] Y. Song, X. Zheng, W. Wang, H. Zhang, B. Zhou, Opt. Lett. 31 (2006) 3234.
[7] T. Ye, Q. Chang, J. Gao, Y. Su, in: Proc. OFC, Paper JWA64, 2008.
[8] J. Yu, Z. Jia, L. Yi, Y. Su, G.K. Chang, T. Wang, IEEE Photon. Technol. Lett. 18 (2006) 265.